ELSEVIER

Chemical Engineering Journal 84 (2001) 533–541

Chemical Engineering Journal

www.elsevier.com/locate/cej

A simulation study of dynamic neural filtering and control of a fed-batch bioreactor under nonideal conditions☆

P.R. Patnaik*

Institute of Microbial Technology, Sector 39-A, Chandigarh 160 036, India

Received 3 October 2000; accepted 3 January 2001

Abstract

Bioreactors utilizing genetically modified bacteria under realistic conditions are difficult to monitor and model because of imperfect mixing, disturbances and uncertain kinetics. In this work, neural filtering and control have been applied to such a nonideal fed-batch bioreactor containing recombinant *Escherichia coli* to produce β-galactosidase. Data simulating industrial fermentation were generated by introducing incomplete mixing in the broth and Gaussian noise in the feed stream. Based on a previous study, an Elman neural network was employed to represent the simulated data. To this, an autoassociative network was added in order to filter the noise and a feed forward network to control the fermentation. Performance of the fermentation with this system of three neural networks optimized together has been shown to be superior to sequential optimization, neural control without filtering, PID control with filtering, and also a noise-free fermentation. Thus, a suitably designed system of neural networks provides rapid on-line estimations and improves bioreactor performance under conditions simulating industrial fermentation.

Keywords: Recombinant fermentation; β-Galactosidase; Neural filtering; Neural control

1. Introduction

Two salient features of ideal bioreactors get diminished on scaling up from laboratory to production scale. One is macroscopic homogeneity of the fermentation broth; in large bioreactors it is difficult to ensure perfect mixing throughout the vessel at all times. The other feature is the intrusion of disturbances in industrial-scale operation. Practical and economic restrictions make it difficult to control large reactors as accurately as small ones. Since disturbances (or process noise) are usually carried by inflow streams, fed-batch and continuous fermentations are more likely to be affected than batch fermentations. However, the kinetics of many fermentations employing genetically modified (recombinant) bacteria are such that better yields of product are obtained in fed-batch and two-stage continuous cultivations than in batch operation [1,2].

The absence of perfect mixing is not necessarily a negative feature of large bioreactors, especially those involving competition between two or more kinds of cells. A recombinant fermentation broth contains two kinds of cells: (a) those containing an externally introduced plasmid and (b) cells without this plasmid. Both types of cells utilize the substrates but only the plasmid-bearing cells can synthesize the desired recombinant protein. In such a competitive environment, the attainable concentration of the protein is maximized by an optimal degree of mixing [3,4], which may vary with time.

Imperfect mixing provides another benefit in fermentations utilizing temperature-sensitive plasmids. These plasmids replicate extremely slowly below a threshold temperature and uncontrollably fast above this temperature. Conventional operation is to run the fermentation for short durations alternately above and below the threshold temperature [5]. By maintaining less than complete mixing in the broth, it is possible to avoid temperature cycling and have isothermal operation below the threshold temperature [6].

Noise carried by the feed stream is a common feature of production scale chemical and biological reactors. Fermentations employing genetically altered bacteria are strongly susceptible to inflow noise, which may change the metabolic pattern, productivity and stability. Traditionally, process noise has been viewed as undesirable, and therefore, many bioreactor operations have tried to eliminate the noise as much as was practically possible [7,8]. This approach has been questioned by a recent study [9], which has shown that allowing disturbances of a prescribed pattern to go through is more beneficial than unregulated noise or the complete

☆ IMTECH communication no. 016/2000.

* Tel.: +91-172-690-223; fax: +91-172-690-585.

E-mail address: pratap@imtech.ernet.in (P.R. Patnaik).

1385-8947/01/$ – see front matter
PII: S1385-8947(01)00126-7

Nomenclature

D	overall dilution rate (h^{-1})
D_a	axial dispersion coefficient (cm^2/h)
D_j	internal dilution rate for j-th region (h^{-1})
k_1, k_2, k_3, k_4	reaction rate constants (h^{-1})
K, K_1, K_2, K_p	equilibrium constants (g/l)
L	characteristic length for bioreactor (cm)
Q	substrate feed rate (1(el)/h)
Q_1	internal flow rate from region (1) to region (2) (1(el)/h)
Q_2	internal flow rate from region (2) to region (1) (1(el)/h)
r^+_{Aj}, r^-_{Aj}	rates of change of A-compartments in j-th region (h^{-1})
r^+_{Gj}, r^-_{Gj}	rates of change of G-compartments in j-th region (h^{-1})
r^+_{Pj}	rate of change of P-compartment in j-th region (h^{-1})
r^+_{Ej}	rate of change of E-compartment in j-th region (h^{-1})
S_f	substrate concentration in the feed stream (g/l(el))
S_0	initial substrate concentration in bioreactor (g/l(el))
S_j	substrate concentration in j-th region (g/l(el))
s_j	S_j/S_0
t	time (h)
u	fluid velocity (cm/h)
V	total volume of the broth (l(el))
V_j	volume of broth in j-th region (l(el))
v_1	V_1/V_0
X	overall biomass concentration in bioreactor (g/l(el))
x	X/S_0
X^+_j	concentration of plasmid-bearing cells in j-th region (g/l(el))
X^-_j	concentration of plasmid-free cells in j-th region (g/l(el))
x^+_j	X^+_j/S_0
x^-_j	X^-_j/S_0
x^+	$x^+_1 + x^+_2$
x^-	$x^-_1 + x^-_2$
x^+_{Aj}, x^-_{Aj}	concentrations of A-compartments in j-th region (g/g)
x^+_{Gj}, x^-_{Gj}	concentrations of G-compartments in j-th region (g/g)
x^+_{Pj}	concentration of P-compartment in j-th region (g/g)
x^+_{Ej}	concentration of E-compartment in j-th region (g/g)
$Y_{x/s}$	yield coefficient for biomass from substrate (g/g)

Greek symbols

Δ_j	Q_j/V_1 (h^{-1})
φ	mass fraction of recombinant cells
γ_{11}, γ_{22}	stoichiometric coefficients for intra-cellular reactions
ω	V_2/V_1
μ	overall specific growth of biomass (h^{-1})
μ^+_j, μ^-_j	specific growth of cells in j-the region (h^{-1})
μ_j	overall specific growth rate in j-th region (h^{-1})
σ^+_j, σ^-_j	intra-cellular substrate concentration in j-th region (g/l(el))
θ	plasmid loss probability
τ	tD

Superscripts

$+$	plasmid-containing cells
$-$	plasmid-free cells

absence of noise. That study extended prior work [10] by prefixing a neural filter to a neural controller, the latter having been shown earlier to provide greater concentrations of recombinant cell mass and its product, β-galactosidase, than adaptive PID control.

One limitation of the two previous studies was that first the controller was optimized for an imperfectly mixed, noise-affected fermentation; this was then coupled to a neural filter and the performance of the bioreactor was determined for different filtered variances of Gaussian noise in the feed stream. However, as Fig. 1 shows, the filter, the controller and the bioreactor are interactive, and therefore, the best performance requires both neural networks (indeed three, as will be explained later) to be designed together and updated continually during the fermentation. This integrated optimization is the subject of the present communication.

2. Problem description

The temperature-sensitive plasmid whose performance has been studied here is pOU140 contained in cells of *Escherichia coli* CSH50. Betenbaugh et al. [5] reported a threshold temperature of 37°C for this plasmid. Below 37°C, the replication rate is too slow to sustain the fermentation; above this temperature the replication rate shoots up so dramatically that the plasmid load soon becomes fatal for the cells. So they proposed operating the fermentation initially above 37°C until a sufficiently large concentration of plasmids is established, but the temperature is lowered

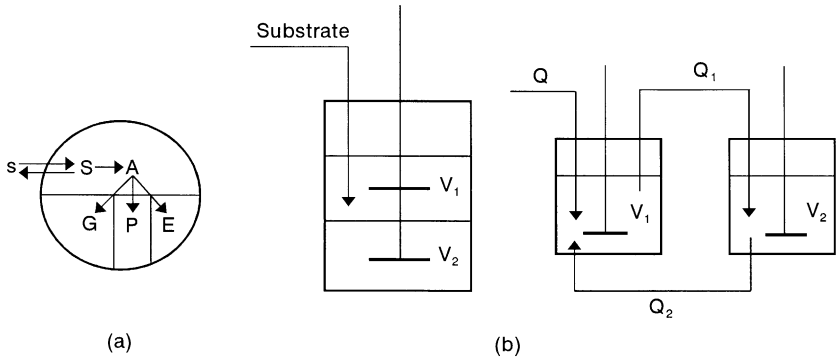

Fig. 1. Schematic diagrams for a structured cell model [11] and its application in a model for fluid mixing in a fed-batch bioreactor [6].

before this reaches a lethal level. The large number of plasmids per cell enables low temperature (below 37°C) fermentation to be carried out for a few hours, after which the temperature is raised again.

To overcome the difficulties of cyclic temperature operation with run-away plasmids, Patnaik [6] proposed controlling the intensity of mixing in such a way as to favor plasmid-bearing cells. This allowed the fermentation to be carried out below 37°C in fed-batch mode for more than 20 h without appreciable loss of plasmid stability. This duration was long enough to reach a practical stationary state. Based on this concept and a kinetic model developed earlier [11], Patnaik [6] formulated a model incorporating imperfect mixing, segregational instability and an impure inoculum (i.e. an inoculum that has some plasmid-free cells). This model, whose equations are presented in Appendix A, was the basis for neural control and neural filtering studies described next. Unlike previous work with this system [5,11], the presence of plasmid-free cells at the beginning of fermentation is both a practical consideration and a theoretical requirement for a sustainable process [12].

The model describes the fermentation at two levels. The intra-cellular reactions are expressed according to the kinetics proposed by Nielsen et al. [11], who divided each cell conceptually into four compartments containing, A: mRNA, tRNA and ribosomes; P: recombinant DNA; E: recombinant protein; and G: genomic DNA and structural material. Mixing in the bioreactor is quantified by visualizing the broth to consist of two regions, with each region feeding the other internally (Fig. 1). Thus, each region functions as a continuous flow reactor, and the broth as a whole operates in fed-batch mode because of the inflow of substrate. Consequently, there are two internal dilution rates, D_1 for region (1) and D_2 for region (2), in addition to an overall dilution rate D. These are defined in Eq. (A.1) of Appendix A.

If D_1 or D_2 is large, that region has intense mixing, while a low dilution rate indicates poor mixing. In the limiting cases, $\{D_1,\ D_2 \to \infty\}$ indicates a perfectly mixed broth, while $\{D_1,\ D_2 \to 0\}$ denotes complete segregation of the two regions. These limits are, however, ideal conditions, and in practical operation D_1 and D_2 have finite non-zero values. Although D also influences mixing, its principal role is in determining the availability of substrate for cellular reactions [6].

The intra-cellular and extra-cellular processes are linked by transport across the cell walls as described by Nielsen and Villadsen [13]. The relevant equations are presented in Appendix A. Previous studies [8,14,15] have shown that inflow noise in a bioreactor may be characterized adequately by a Gaussian distribution. So the reactor model in Eqs. (A.12)–(A.18) was 'corrupted' by adding noise with a variance of 8% of the inlet flowrate and concentration. This variance has been shown earlier [9] to maximize β-galactosidase activity. The coupled equations for intra-cellular kinetics and bioreactor dynamics were solved both without and with noise; the initial dilution rates were set at optimum values determined earlier [6]: $D_1 = D_2 = 0.3\,\mathrm{h}^{-1}$; $D = 0.1\,\mathrm{h}^{-1}$.

Data generated by the model represented a simulated industrial fermentation. The simulated plant has experimental validity because the kinetics, the mixing model and Gaussian distribution for noise have all been separately verified. Because practical and commercial difficulties limit the data that can be obtained from an industrial bioreactor, many authors [14,16–18] have recommended the use of simulated data from a combination of experimentally validated models. This approach also allows plant performance to be simulated under a variety of conditions so that appropriate control strategies may be developed.

3. Neural filtering and control

Because practical difficulties and sometimes proprietary restrictions limit the exploration of industrial bioreactors under disturbed conditions, many authors [14,16,17] have found it useful to simulate the behavior by applying disturbances to a model of an ideal bioreactor. Adopting this approach, Patnaik [10,15] added Gaussian noise in the flow rate of the feed stream of a model developed earlier [6] in order to generate data mimicking an industrial-scale fermentation. These data were then considered to represent a simulated

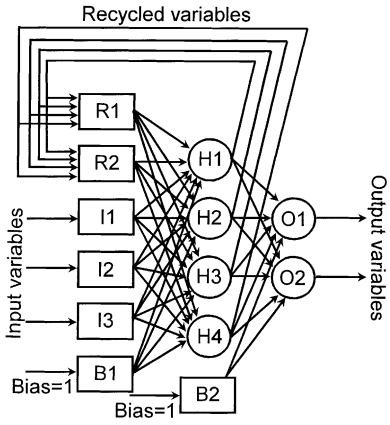

Fig. 2. Structure of an Elman neural network. Input neurons: I1, I2 and I3; output neurons: O1 and O2; hidden neurons: H1, H2, H3 and H4; bias neurons: B1 and B2; recurrent neurons: R1 and R2.

nonideal bioreactor and a neural network was designed to portray the performance. In a practical context, the network would simulate real data from an operating bioreactor.

As discussed before [15], feed forward networks with prefixed filtering devices [8] are a contrived and often inadequate method to depict a dynamic process such as fed-batch fermentation, and they can result in significant overparameterization [19]. A neural network with internal feedback provides a more natural representation of fermentation dynamics with internal recycles of the kind shown in Fig. 1. Given a neural network with an input layer, a hidden layer and an output layer, one may provide recycle of information to the input layer from either the output layer or the hidden layer. The former design is called a Jordan network and the latter an Elman network [20]. Because the recycle streams in mixing models such as Fig. 1 are within the system, the Elman configuration (Fig. 2) has greater fidelity to the actual situation. This type of network has been shown [15] to represent β-galactosidase fermentation in the presence of both random noise and large disturbances better than a feed forward ANN and the radial basis ANN employed by Thompson and Kramer [17]. Details of how the Elman ANN is trained have been described elsewhere [15,19].

The interactions are both physiological and physical. Physiological interactions are evident from the dependence of the specific growth rate on intra-cellular concentrations (Eqs. (A.4), (A.7) and (A.8)) and of the substrate concentration in the bioreactor on the specific growth rate (Eqs. (A.17) and (A.18)). The physical interactions gain significance with increasing size of the reaction vessel. In a small reactor, nearly complete mixing is achieved, whereas in large reactors there are significant differences even on a microscopic scale [21]. The spatial gradients affect the chemotactic movements of recombinant cells and plasmid-free cells, dispersion of cells and substrate, and consequently, the accessibility of substrate to both kinds of cells [6]. Since quantifying these effects by a mathematical model is difficult and requires intricate measurements, a recurrent neural network may be trained to portray the physical interactions without requiring detailed measurements or a detailed model.

Coupling this recurrent network to a feed forward neural controller generated better performance than was possible with adaptive PID control [10]. Therefore, a follow-up study [9] extended this work in two ways. Firstly, the Gaussian noise was considered to have components of different variances rather than the single variance considered earlier. Each component has a time-dependent mean equal to the instantaneous value of the flow rate. This is more closely representative of a real situation [8,19,22]. Secondly, a neural filter was added prior to the controller so as to prune the variance of the disturbances. Since the inputs and outputs of the filter are the same, an autoassociative network was chosen according to previous recommendations [15,19,23]. The network was trained to allow noise of a prescribed variance to go through with the feed stream.

The filtering study showed that the peak concentration of β-galactosidase attainable with a neural filter was larger than with a static filter or even in the absence of noise. Although coupling of a neural filter to a neural controller improved β-galactosidase production, this could not be said to be the maximum possible because of two reasons. First, the two networks had been optimized separately, first for control [10] and then for filtering [9]. Secondly, the variance of the disturbances that was allowed to pass through the filter was the same throughout the fermentation; this may not be a good approximation because in a real situation it is not known in advance how widely the components of the noise differ in their variances. So these limitations have been relaxed in the present simulation. The neural networks representing the filter, the controller and the bioreactor were optimized during each interval of time according to the flowsheet in Fig. 3, and the best variance during each interval was determined as that which maximized the β-galactosidase concentration during that period. This allowed the optimal variance to be a function of time.

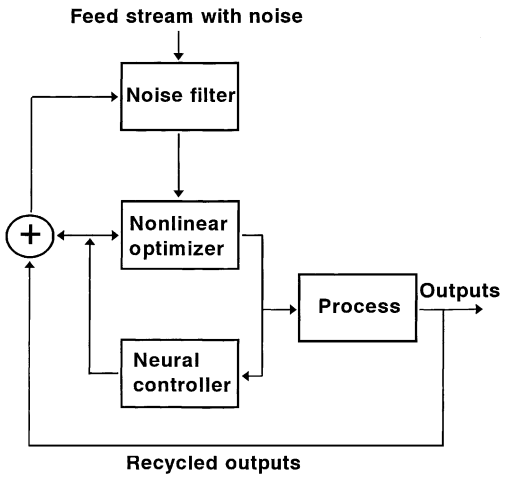

Fig. 3. Information flow diagram for neural filtering and control of a bioreactor.

4. Results and discussion

This communication presents results for a simulated fed-batch β-galactosidase fermentation where the complete neural system was optimized over short successive intervals of time until the end of fermentation. Fig. 3 depicts the logic diagram. Whereas the "process" box would normally denote a bioreactor, here it contains an equivalent Elman neural network [15]. As explained before [9,10], the controller was a feed forward network and the filter an autoassociative network. Even though a feed forward network is easy to design, an autoassociative configuration is germane to the functioning of the filter, which has the same inputs and outputs. The duration of fermentation (20 h) was discretized into intervals of 0.5 h and the weights of the three neural networks were computed during each time interval so as to maximize β-galactosidase concentration during that interval, using data at the end of the preceding interval as the initial condition. This Markovian policy was chosen because it has provided stable fermentations with high activities of the recombinant protein for many *E. coli* strains [8,10,24].

In fermentations with recombinant *E. coli*, maximization of the concentration of the cloned-gene protein, β-galactosidase, requires a high concentration of recombinant cells [1,2]. So the time-domain profiles of these two variables provide a good indication of the effects of control and filtering. These profiles have been plotted in Figs. 4 and 5 for four situations: (1) without filtering and control; (2) with neural control but no filtering of noise; (3) with neural filtering and control, but with the two neural networks being optimized separately and (4) with both neural networks (and that for the bioreactor) being optimized together.

In the absence of control of the bioreactor and filtering of noise, the concentrations of recombinant cells and their product decrease initially and begin to rise after 5 h. The decrease of β-galactosidase concentration (Fig. 5) is much larger

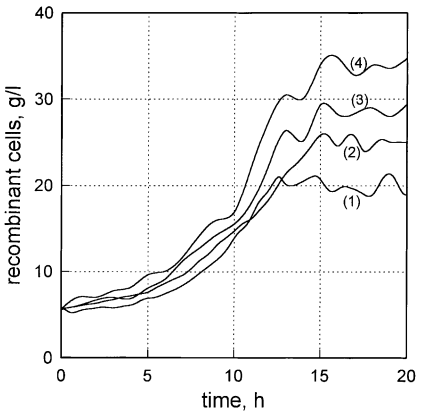

Fig. 4. Evolution of the concentration of recombinant cells with time for (1) uncontrolled fermentation: (2) neural control without filtering of noise; (3) with neural filtering and control but with the networks optimized separately; (4) integrated optimization of neural filter, neural controller and the bioreactor.

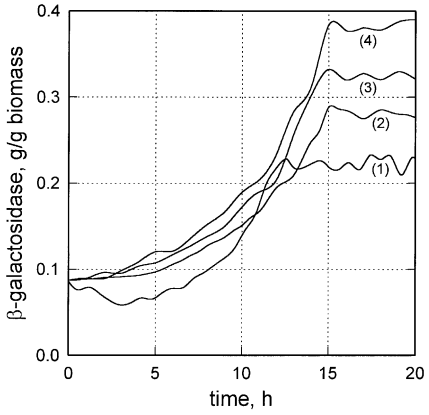

Fig. 5. Evolution of β-galactosidase concentration with time for the four cases shown in Fig. 4.

than might be expected from that of plasmid-harboring cells (Fig. 4). This implies that noise affects the internal metabolism and the structural stability of the plasmid, whereas deterministic models [4,6] have expressed only segregational instability. This effect of noise is compatible with the cell model in Fig. 1. Thorough the RNA and ribosomes of compartment A, the inflow substrate affects the stability of rDNA (compartment P) and expression of the recombinant protein (compartment E).

The increase in the concentrations after a length of time and the eventual "constant" maxima have been explained elsewhere [6,10] and are briefly recapitulated here. Plasmid-harboring cells grow flagellae and streamline their shape [25], which help their movement through the fermentation broth. As shown in Fig. 1, the inoculum is injected into one region and allowed to disperse throughout. Thus, initially the inoculated region has both plasmid-bearing and plasmid-free cells in low concentrations and, because of the moderate degree of mixing ($D_1 = D_2 = 0.3\,h^{-1}$), the other region is almost devoid of cells. The practical implication of this conceptual demarcation is the existence of regions of cell-free substrate and concentrated pockets of cells with inadequate accessibility to substrate. This impedes growth and protein synthesis, causing the initial decrease in their concentrations (Figs. 4 and 5). Eventually, however, the faster motion of plasmid-harboring cells promotes their homogeneous distribution, mixing has reached an optimum level and there is sufficient inflow of substrate. Owing to these factors and the larger spatially averaged concentrations perceived by plasmid-containing cells in an imperfectly mixed broth [26], there is better utilization of substrate and consequent increase in the concentrations. Because of metabolic limitations and competition with plasmid-free cells, the concentrations stabilize after a certain length of time.

Table 1 compares the "steady-state" performance of the bioreactor under different conditions. As seen in Figs. 4 and 5, strictly constant outputs are not achieved because of variable mixing in the broth and the influx of noise. So the data reported are the values averaged from the 15th

Table 1
Comparison of bioreactor performance under different methods of operation

Performance indicator	Uncontrolled (absolute values)	Neural control without filtering (% increase)	Separate control and filtering (% increase)	Combined control and filtering (% increase)
Recombinant cells (g/l)	19.81	26.75[a]	45.03[a], 14.42[b]	71.58[a], 18.31[b]
β-Galactosidase (g/g biomass)	0.222	27.03	46.40, 15.25	72.52, 17.85
β-Galactosidase (g/l)	0.285	22.16	38.60, 13.51	58.59, 14.43

[a] Percentage increase over uncontrolled fermentation.
[b] Percentage increase over the preceding column.

to the 20th hour, when reasonably steady oscillations are observed. Compared to uncontrolled fermentation, an integrated neural system optimized dynamically achieved more than 70% increase in recombinant cell mass concentration per unit volume of broth and in β-galactosidase production per unit cell mass. The addition of a neural filter to a neurally controlled bioreactor enhanced β-galactosidase concentration by 15% when the two were optimized sequentially and by a further 18% when optimized together with the bioreactor model. The effects of other types of filtering and of adaptive PID control are not shown because it has been demonstrated earlier [9] that they are inferior to a combination of neural networks.

The somewhat smaller increases in β-galactosidase concentration per unit volume of broth (Table 1) may be attributed to the more sluggish response of the mass fraction of recombinant cells (not shown) compared to their concentration. Plasmid-containing cells respond more slowly to a disturbance than plasmid-free cells do [27]. Consequently, there is a larger percentage change in the concentration of plasmid-free cells, and this reduces the change in the mass fraction. Since conversion of β-galactosidase concentration per unit cell mass to a volumetric unit requires division by the mass fraction, the improvements reflected in the last three columns of Table 1 become moderated. Nevertheless, the enhancement of performance is substantial even in volumetric terms. This may be attributed to resonance between the natural frequency of the process and the controlled frequency of noise in the filtered feed stream. However, the natural frequency may change with time in a fed-batch fermentation because of continual changes in volume, cell concentrations and rheological properties. Hence, the earlier attempt [9] to seek the best constant variance in the outlet of the filter is restrictive and sub-optimal. Relaxing this restriction in the present study, the variance which maximizes β-galactosidase concentration was determined for each interval (0.5 h) of time. This is seen to increase from 5.3 to 8.0% during the span of 20 h (Fig. 6), a change of more than 50%. Thus, it is not reasonable to design a neural filter for a constant variance. While this appears to be the first report of a time-dependent optimal variance, constant optimal variances for other organisms and products [28,29] support the inference from β-galactosidase that a neural filtering and control configuration is superior to conventional methods for rapid on-line estimations and control of recombinant fermentations under nonideal conditions.

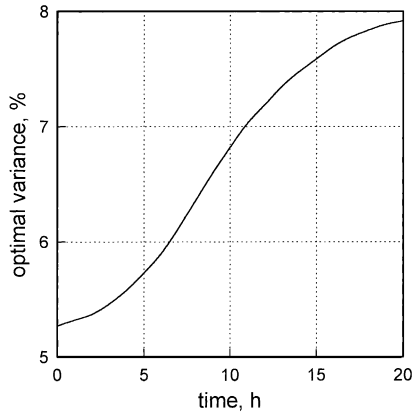

Fig. 6. Variation of the optimal variance of filtered noise with time for a bioreactor optimized on-line by a neural filter and a neural controller as in case (4) of Figs. 4 and 5.

5. Conclusions

Recombinant fermentations carried out under production conditions are difficult to model and are susceptible to noise carried by the feed stream. Previous work [9,10,29] had expressed the noise by a Gaussian distribution and it had been shown that controlled filtering of noise resulted in greater concentrations of the recombinant protein (β-galactosidase) than no filtering or complete removal of noise.

Extending those studies, in this work the noise has been characterized by a set of Gaussian distributions with time-dependent means and variances. Three neural networks were employed — one for filtering, one for control and a third for the fermentation itself. While neural control without filtering of noise and a combination of filtering and control optimized separately achieved increases between 22 and 46% in β-galactosidase concentration, this could be enhanced to nearly 60% (for concentrations in g/l) and 72% (in g/g biomass) by optimizing the three neural nets dynamically as shown in Fig. 3. The optimal variance of the filtered noise increased by more than 50% during the 20 h fermentation, suggesting that earlier attempts [9,29] to maintain the same concentration throughout might have been too approximate.

These observations suggest four inferences:

1. Inflow noise prevalent in large bioreactor operations is more appropriately characterized by a mixture of

Gaussian distributions than by a single distribution.
2. Neural networks may be used to represent a nonideal bioreactor, filter any disturbances continually and control the fermentation.
3. Substantial improvement in the simulated β-galactosidase concentration is possible by optimizing an autoassociative neural network for controlled filtering, a feed forward network for on-line control and a recurrent network for the bioreactor in a dynamic loop.
4. Because of the limitations of mathematical models and measurement devices for large bioreactors, neural networks offer a convenient and rapid method for on-line estimations and control even under disturbed conditions.

Appendix A

Patnaik [6] modified the equations proposed by Nielsen et al. [11] to make them applicable for fed-batch operation with plasmid-bearing cells present in the starting culture and segregational instability. The broth is visualized to consist of two regions, each functioning as a separate bioreactor (Fig. 1). Internal recycle streams connect the reactors to represent fluid circulation. Mixing is characterized by three dilution rates, defined below

$$D_1 = \left(\frac{Q + Q_2 - Q_1}{V_1}\right), \qquad D_2 = \left(\frac{Q_1 - Q_2}{V_2}\right) \tag{A.1}$$

where Q's denote the flow rates and V_1, V_2 are the volumes of broth in the two conceptual reactors. Metabolic reactions take place inside the recombinant cells, there is partial reversion of plasmid-bearing cells to plasmid-free cells, and transport processes link the intra-cellular reactions to the extra-cellular broth.

A.1. Kinetic equations inside the cells

A.1.1. Plasmid-bearing cells

$$\begin{bmatrix} \dfrac{dx^+_{Aj}}{dt} \\ \dfrac{dx^+_{Gj}}{dt} \\ \dfrac{dx^+_{Pj}}{dt} \\ \dfrac{dx^+_{Ej}}{dt} \end{bmatrix} = \frac{1}{D}\begin{bmatrix} \gamma_{11} & -1 & -1 & -1 \\ 0 & \gamma_{22} & 0 & 0 \\ 0 & 0 & \gamma_{22} & \gamma_{22} \\ 0 & 0 & 0 & \gamma_{22} \end{bmatrix}\begin{bmatrix} r^+_{Aj} \\ r^+_{Gj} \\ r^+_{Pj} \\ r^+_{Ej} \end{bmatrix} - \frac{\mu^+_j}{D}\begin{bmatrix} x^+_{Aj} \\ x^+_{Gj} \\ x^+_{Pj} \\ x^+_{Ej} \end{bmatrix} \tag{A.2}$$

where

$$\begin{bmatrix} r^+_{Aj} \\ r^+_{Gj} \\ r^+_{Pj} \\ r^+_{Ej} \end{bmatrix} = \begin{bmatrix} \dfrac{k_1\sigma^+_j x^+_{Aj}}{(\sigma^+_j + K_1)} \\ \dfrac{k_2\sigma^+_j x^+_{Aj}}{(\sigma^+_j + K_2)} \\ \dfrac{k_3\sigma^+_j x^+_{Aj} x_n}{(\sigma^+_j + K_2)} \\ \dfrac{k_4\sigma^+_j x^+_{Aj} x^+_{Pj}}{(\sigma^+_j + K_2)(x^+_{Pj} + K_P)} \end{bmatrix} \tag{A.3}$$

The specific growth rate is

$$\mu^+_j = \gamma_{11} r^+_{Aj} - (1 - \gamma_{22})(r^+_{Gj} + r^+_{Pj} + r^+_{Ej}) \tag{A.4}$$

A.1.2. Plasmid-free cells

$$\begin{bmatrix} \dfrac{dx^-_{Aj}}{dt} \\ \dfrac{dx^-_{Gj}}{dt} \end{bmatrix} = \begin{bmatrix} \gamma_{11} & -1 \\ 0 & \gamma_{22} \end{bmatrix}\begin{bmatrix} r^-_{Aj} \\ r^-_{Gj} \end{bmatrix} - \frac{\mu^-_j}{D}\begin{bmatrix} x^-_{Aj} \\ x^-_{Gj} \end{bmatrix} \tag{A.5}$$

Similar to Eqs. (A.3) and (A.4), we may write

$$\begin{bmatrix} r^-_{Aj} \\ r^-_{Gj} \end{bmatrix} = \begin{bmatrix} \dfrac{k_1\sigma^-_j x^-_{Aj}}{(\sigma^-_j + K_1)} \\ \dfrac{k_2\sigma^-_j x^-_{Aj}}{(\sigma^-_j + K_2)} \end{bmatrix} \tag{A.6}$$

and

$$\mu^-_j = \gamma_{11} r^-_{Aj} - (1 - \gamma_{22}) r^-_{Gj} \tag{A.7}$$

In these equations, the superscript (+) denotes cells containing the plasmid, superscript (−) denotes cells without the plasmid, and the subscript j equals 1 or 2, depending on which mixing region is being analyzed. Eqs. (A.5) and (A.6) do not contain concentrations and rates for the P- and E-compartments because they are not present in non-recombinant (plasmid-free) cells.

The overall specific growth rate of biomass in each region is the weighted sum of the growth rates for the two kinds of cells

$$\mu_j = \left(\frac{x^+_j}{x^+_j + x^-_j}\right)\mu^+_j + \left(\frac{x^-_j}{x^+_j + x^-_j}\right)\mu^-_j \tag{A.8}$$

Conservation equations relate the intra-cellular components to the overall concentrations of plasmid-free and plasmid-bearing cells.

$$x^+_{Aj} + x^+_{Pj} + x^+_{Gj} + x^+_{Ej} = x^+_j, \quad j = 1 \text{ or } 2 \tag{A.9}$$

$$x^-_{Aj} + x^-_{Gj} = x^-_j, \quad j = 1 \text{ or } 2 \tag{A.10}$$

The intra-cellular substrate concentrations, σ^+_j and σ^-_j, may also be related to the concentrations, S_j, in the medium. This,

however, is not straightforward like Eqs. (A.9) and (A.10). The method has been described by Nielsen and Villadsen [13], and it leads to

$$\sigma_j^+ = \sigma_j^- = \frac{kK_1S_j}{k_1(S_j + K)}, \quad j = 1 \text{ or } 2 \tag{A.11}$$

A.2. Bioreactor model

$$\frac{dv_1}{d\tau} = v_1 \tag{A.12}$$

$$\frac{dx_1^+}{d\tau} = \frac{Y_{x/s}}{\mu x}[\mu_1^+ x_1^+(1-\theta) + \Delta_2 x_2^+ - \Delta_1 x_1^+] - x_1^+ \tag{A.13}$$

$$\frac{dx_1^-}{d\tau} = \frac{Y_{x/s}}{\mu x}[\mu_1^+ x_1^+\theta + \mu_1^- x_1^- + \Delta_2 x_2^- - \Delta_1 x_1^-] - x_1^- \tag{A.14}$$

$$\frac{dx_2^+}{d\tau} = \frac{Y_{x/s}}{\mu x}\left[\mu_2^+ x_2^+(1-\theta) + \frac{(\Delta_1 x_1^+ - \Delta_2 x_2^+)}{\omega}\right] - x_2^+ \tag{A.15}$$

$$\frac{dx_2^-}{d\tau} = \frac{Y_{x/s}}{\mu x}\left[\mu_2^+ x_2^+\theta + \mu_2^- x_2^- + \frac{(\Delta_1 x_1^- - \Delta_2 x_2^-)}{\omega}\right] - x_2^- \tag{A.16}$$

$$\frac{ds_1}{d\tau} = (1+\omega)s_f + \frac{Y_{x/s}}{\mu x}(\Delta_2 s_2 - \Delta_1 s_1) - s_1 \tag{A.17}$$

$$\frac{ds_2}{d\tau} = \frac{Y_{x/s}}{\omega\mu x}(\Delta_1 s_1 - \Delta_2 s_2) \tag{A.18}$$

Eqs. (A.13)–(A.18) incorporate the optimum dilution rate for fed-batch fermentations [1,13], $D = \mu x / Y_{x/s}$. Since x and μ, specified by Eqs. (A.20) and (A.21), vary as fermentation progresses, so does D. There is no conservation equation for β-galactosidase because it is retained inside the cells.

From a mass balance for V_2, it can be shown that

$$\Delta_1 - \Delta_2 = \omega D \tag{A.19}$$

The total cell mass concentration (x) is calculated as

$$x = x_1^+ + x_1^- + x_2^+ + x_2^- \tag{A.20}$$

and the overall specific growth rate is the volumetrically weighted sum of the growth rates in the two regions

$$\mu = \left(\frac{\mu_1 + \omega\mu_2}{1+\omega}\right) \tag{A.21}$$

The individual specific growth rates, μ_j^+, μ_j^- and μ_j with $j = 1$ or 2, are computed according to Eqs. (A.4), (A.7) and (A.8).

References

[1] K. Friehs, K.F. Reardon, Parameters influencing the productivity of recombinant *E. coli* cultivations, Adv. Biochem. Eng. 48 (1993) 54–77.

[2] L. Yee, H.W. Blanch, Recombinant protein expression in high cell density fed-batch cultures of *Escherichia coli*, Bio. Technol. 10 (1992) 1550–1556.

[3] P.R. Patnaik, Micromixing and the steady-state performance of bioreactors using recombinant bacteria — analysis through a two-environment model, J. Chem. Technol. Biotechnol. 61 (1994) 337–342.

[4] P.R. Patnaik, Plasmid stability analysis in a non-homogeneous bioreactor for a fed-batch recombinant fermentation, Can. J. Chem. Eng. 77 (1999) 602–607.

[5] M.J. Betenbaugh, V.M. diPasquantonio, P. Dhurjati, Improvement of product yields by temperature-shifting of *Escherichia coli* cultures containing plasmid pOU140, Biotechnol. Bioeng. 29 (1987) 513–519.

[6] P.R. Patnaik, Dispersion-induced behavior in sub-critical operation of a recombinant fed-batch fermentation with run-away plasmids, Bioprocess Eng. 18 (1998) 219–226.

[7] P. Grainordge, S. Carbonnier, J.P. Magnin, C. Mauvy, A. Cheruy, A software sensor of biological activity based on a redox probe for the control of *Thiobacillus ferrooxidans* cultures, J. Biotechnol. 35 (1994) 87–96.

[8] J. Glassey, G.A. Montague, A.C. Ward, B.V. Kara, Enhanced supervision of recombinant *E. coli* fermentations via artificial neural networks, Process Biochem. 29 (1994) 387–398.

[9] P.R. Patnaik, Coupling of a neural filter and a neural controller for improvement of fermentation performance, Biotechnol. Tech. 13 (1999) 735–738.

[10] P.R. Patnaik, Neural control of an imperfectly mixed bioreactor for recombinant β-galactosidase, Biochem. Eng. J. 3 (1999) 113–120.

[11] J. Nielsen, A.G. Pedersen, K. Strudsholm, J. Villadsen, Modeling fermentations with recombinant microorganisms: formulation of a structured model, Biotechnol. Bioeng. 37 (1991) 802–808.

[12] S.-B. Hsu, P. Waltman, G.S.K. Wolkowicz, Global analysis of a model of plasmid-bearing, plasmid-free cells in a chemostat, J. Math. Biol. 32 (1994) 731–742.

[13] J. Nielsen, J. Villadsen, Modeling of microbial kinetics, Chem. Eng. Sci. 47 (1992) 4225–4270.

[14] R. Simutis, A. Lubbert, Exploratory analysis of bioprocesses using artificial neural network based methods, Biotechnol. Prog. 13 (1997) 479–487.

[15] P.R. Patnaik, A recurrent neural network for a fed-batch fermentation with recombinant *Escherichia coli* subject to inflow disturbances, Process Biochem. 32 (1997) 391–400.

[16] J. Thibault, V. van Breusegem, A. Cheruy, On-line prediction of fermentation variables using neural networks, Biotechnol. Bioeng. 36 (1990) 1041–1048.

[17] M.L. Thompson, M.A. Kramer, Modeling chemical processes using prior knowledge and neural networks, AIChE J. 40 (1994) 1328–1340.

[18] J. Schubert, R. Simutis, M. Dors, I. Havlik, A. Lubbert, Bioprocess optimization and control: application of hybrid modeling, J. Biotechnol. 35 (1994) 51–68.

[19] G.A. Montague, A.J. Morris, Neural network contributions in biotechnology, Trends Biotechnol. 12 (1994) 312–324.

[20] J.A. Freeman, Simulating Neural Networks with Mathematica. Addison-Wesley, New York, 1994 (Chapter 6).

[21] G. Larsson, M. Tornquist, E.S. Wernersson, C. Tragardh, H. Noorman, S.-O. Enfors, Substrate gradients in bioreactors: origin and consequences, Bioprocess Eng. 14 (1996) 281–289.

[22] G.A. Montague, A.J. Morris, M.T. Tham, Enhancing bioprocess operability with generic software sensors, J. Biotechnol. 25 (1992) 183–204.

[23] T. Masters, Practical Neural Recipes in C++, Academic Press, San Diego, CA, 1993.
[24] K. Ye, S. Jin, K. Shimizu, Fuzzy neural network for the control of high cell density cultivation of recombinant *Escherichia coli*, J. Ferment. Bioeng. 77 (1994) 663–673.
[25] W.D. Stein, F. Bronner, Cell Shape. Determinants, Regulation and Regulatory Role, Academic Press, San Diego, CA, 1989.
[26] P.R. Patnaik, Does macromixing affect plasmid stability during continuous fermentation with recombinant bacteria, Indian Chem. Eng. 36 (1994) 85–88.
[27] M.L. Stephens, G. Lyberatos, Effect of cycling on the stability of plasmid-bearing microorganisms in continuous culture, Biotechnol. Bioeng. 31 (1988) 464–469.
[28] P.R. Patnaik, Fractal characterization of the effect of noise on biological oscillations: the biosynthesis of ethanol, Biotechnol. Tech. 8 (1994) 419–424.
[29] P.R. Patnaik, Improvement of the microbial production of streptokinase by controlled filtering of process noise, Process Biochem. 35 (1999) 309–315.